

An Integrated Optimization-Game Theory Model for CPT-based Subground Stratification

M.S. Farhadi¹

¹*Project Researcher, faculty of Built Environment, Tampere University, Finland. Email: mohammadsadegh.farhadi@tuni.fi*

Abstract: In this study, an integrated Grey Wolf Optimizer (GWO)-Nash-Harsanyi bargaining model was developed for estimating the underground stratification based on the CPT data. For this purpose, the Robertson chart (1990) was utilized to estimate the Soil Behavior Type (SBT) using the normalized cone resistance, Q_m , and normalized friction ratio, F_r , data. Hence, the equations representing the lines in the chart were determined at first. Besides, it was observed that categorizing soils merely according to the Robertson chart's zones included too many uncertainties and noises. Therefore, the outliers' and uncertainties' impact in the two data sets, i.e. F_r and Q_m , was relaxed mainly by means of the Locally Estimated Scatterplot Smoothing (LOESS) method. Next, some simple ordinal distance classes between the points, named as N-H distance criteria, d_{N-H} , were defined and employed in the Nash-Harsanyi Game Theory model as decision-makers. The N-H distance criteria for each point were compared with another factor, defined as α -cut distance criterion, $D_{\alpha-cut}$. Based on an experts' CPT interpretation of stratification, $D_{\alpha-cut}$ and the cooperation of each decision-maker in the Nash-Harsanyi bargaining model were optimized by means of the Grey Wolf Optimizer (GWO) integrated with the Nash-Harsanyi model. The estimated CPT-based stratification was almost similar to the experts' stratification.

Keywords: Subground stratification, CPT, Outliers and uncertainties, Nash-Harsanyi bargaining model, Grey Wolf Optimizer.

1. Introduction

Cone Penetration Test (CPT) has been used and studied for a long time because of its benefits over the other soil investigation methods. It is fast, repeatable, economical, and it provides almost continuous data (Lunne et al., 1986; Robertson, 2009). But the results interpretation is complex and numerous studies have addressed it during the past decades (Lunne, 1986; Robertson, 1990, 2009; Woollard et al., 2016). The present study has targeted the subground stratification based on the CPT data; which has been previously performed based on the basics of geotechnical engineering (Tonni and Gottardi, 2011), the statistical or probabilistic (Jung et al., 2008; Wang et al., 2013), or Artificial Intelligence (AI) methods (Das and Basudhar, 2009; Ching et al., 2015; Cao et al., 2018). An AI-based model was developed in this study to identify the subground layers.

Zhang and Tumay, (1999) suggested the statistical and fuzzy sublayers identification approaches using the soil types almost similar to the ones in the Unified Soil Classification System (USCS). Hegazy and Mayne (2002)

presented the improvement of clustering methods over the statistical ones for the CPT-based soil classification. They showed that clustering could detect major changes within the stratigraphy, which might not be apparently visible. A probabilistic approach was developed by Jung et al. (2008) to modify the soil identification charts based on the CPT data. Das and Basudhar (2009) proposed self-organizing maps and fuzzy clustering techniques for identification of different layers. Wang et al. (2013) modelled the uncertainty in the CPT-based soil classification using the Robertson chart (1990) by means of the Bayesian approaches. The proposed model was evaluated based on some real CPT data. Ching et al. (2015) used the wavelet transform modulus maxima (WTMM) method for stratification based on the Soil Behaviour Type (SBT) Index, I_c . The method was capable of detecting thin soil layers. Li et al. (2016) developed a probabilistic method to predict soil stratification at unsampled locations by estimating the CPT parameters using an established Kriging interpolation technique. Cao et al. (2018) developed a

Bayesian framework based on the SBT Index, I_c , for the probabilistic soil stratification. It estimated the number and thickness of layers, and their associated identification uncertainty.

Uncertainty has an influential role in the interpretation of CPT results. Variations in the mechanical and electrical features of piezometers, tolerances, and the inherent soil variability may lead to different results of tip and specifically sleeve resistances (Lunne et al., 1986; Robertson, 1990). Hence, in this study, a local regression method was utilized to relax the outliers' and uncertainties' impact, and the Nash-Harsanyi bargaining and Grey Wolf Optimizer (GWO) models were integrated for estimating the subground stratification based on the CPT results. The soil type classification is built on the Robertson chart (1990). The proposed framework and its application to some CPT results are described in the following sections.

2. The proposed framework

Recognition of the subground stratification based on the CPT results was performed utilizing the Locally Estimated Scatterplot Smoothing (LOESS) method and the game theory (Nash-Harsanyi bargaining model)

integrated with the GWO model. A concise flowchart of the proposed model is presented in Fig. 1.

2.1. Robertson chart digitization

Robertson (1990) categorized soils, with respect to worldwide CPT results, based on their particles size and their behaviour (Fig. 2). As can be seen, nine classes of soils were defined in the chart.

The boundaries among the soil (behaviour) types in the Robertson chart were identified based on the experiments. Therefore, in order to consider them in calculations, there was no way but to fit curves to the boundary lines. Jung et al. (2008) fitted the exponential equations to curves in a semi-logarithmic space. However, in the present study, both polynomial and exponential equations were fitted to the boundary lines in linear and log-log spaces. Sum Squared Error (SSE), coefficient of determination (R-squared), and Root Mean Square Error (RMSE) were used as the error criteria to compare the fitted curves. The best-fitted equations for each line (numbered on the Robertson chart in Fig. 1) is presented in Table 1.

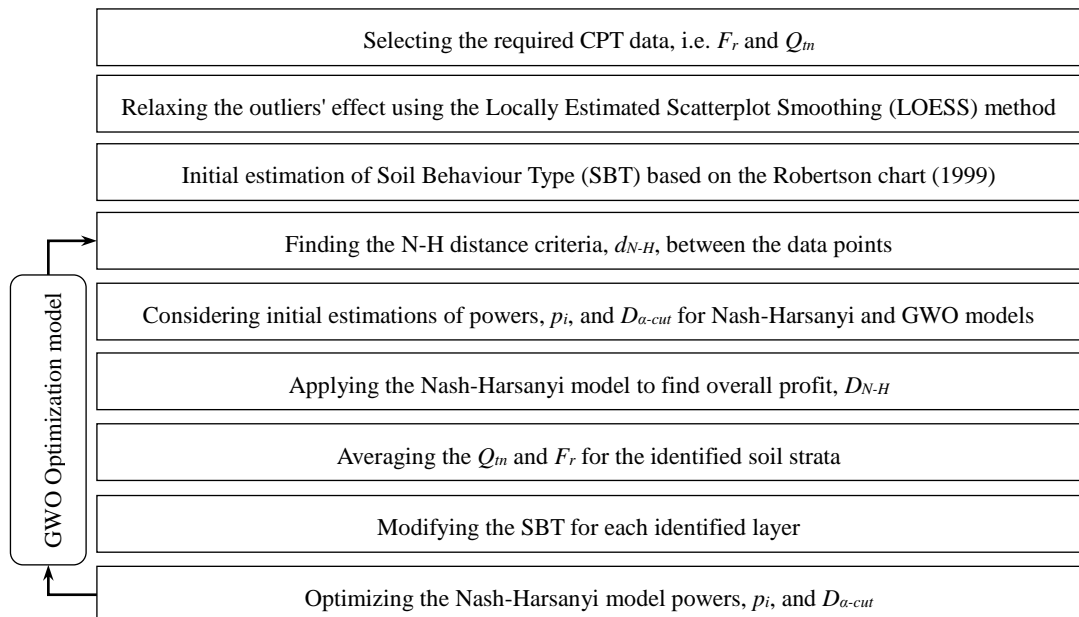
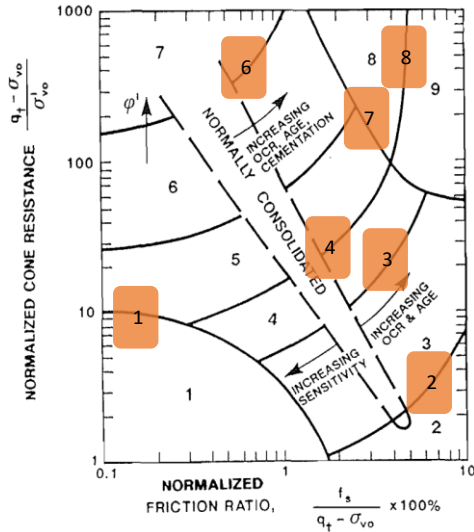


Figure 1: The concise flowchart of the proposed model



Region	Soil behaviour type
1	sensitive, fine grained
2	organic soils-peats
3	clays-clay to silty clay
4	silt mixtures-clayey silt to silty clay
5	sand mixtures-silty sand to sandy silt
6	sands-clean sand to silty sand
7	gravelly sand to sand
8	very stiff sand to clayey sand*
9	very stiff, fine grained*

* Heavily overconsolidated or cemented

Figure 2: Soil Behaviour Type (SBT) chart based on CPT data, proposed by Robertson (1990)

2.2. Relaxing the uncertainties' and outliers' impact

The uncertainties and outliers existence in CPT data is almost inevitable. Numerous studies addressed the outliers detection in time series

(Abraham and Chuang, 1989; Ljung, 1993) and in geotechnical engineering (D'Ignazio et al., 2016; Ching et al., 2018).

Firstly, the SBT chart was drawn according to the Robertson chart for a CPT log results, shown in Fig. 3. Outliers and the consequent SBT fluctuations/noises with different ranges of severity are clearly visible. In order to relax the noises observed on the initial classification based on the Robertson chart, a smoothing method based on the local regression was employed. Smoothing methods have been widely used to estimate trends in economic time series (Macaulay, 1931; Anderson, 1971; Kendall and Ord, 1990; Loader, 1999). Smoothing methods allow the data points themselves to determine the form of the fitted curve. There are several different smoothing approaches, including kernel methods, local regression, spline methods, and orthogonal series (Loader, 2012).

Robust locally weighted regression is a method for smoothing a scatterplot, (x_i, y_i) , $i=1,2,\dots,n$, in which the fitted value at x_k is the value of a polynomial fit to the data using weighted least squares (Cleveland, 1979).

The underlying principle is that a smooth function can be well approximated by a low degree polynomial in the neighborhood, $(-h, h)$, of any point x . For example, a local linear approximation is:

$$\mu(x_i) \approx a_0 + a_1(x_i - x) \quad (1)$$

for $x-h < x_i < x+h$. A local quadratic approximation, which was used in this study, is:

Table 1: The best fitted curves to the Roberson chart boundaries

Line No.	Equation	SSE	R-square	RMSE
1	$y = -2.474x^5 - 7.17x^4 - 7.066x^3 - 3.836x^2 - 1.721x + 0.4744$	0.0012	0.9995	0.00646
2	$y = 1.086x^4 - 0.8107x^3 - 0.09045x^2 + 0.8637x - 0.1521$	0.0004	0.9998	0.00352
3	$y = 0.4864x^3 + 0.2955x^2 + 0.7638x + 0.7346$	0.0023	0.9996	0.00768
4	$y = 1.204 \exp(0.5827x) + 0.0034 \exp(8.784x)$	0.0017	0.9997	0.00650
5	$y = 0.7409x^4 + 1.503x^3 + 1.286x^2 + 0.8894x + 1.806$	0.0022	0.9995	0.00655
6	$y = 0.5231x^3 + 1.518x^2 + 1.743x + 2.924$	0.0016	0.9995	0.00587
7	$y = -0.429x^4 - 1.195x^3 + 5.555x^2 - 6.068x + 3.917$	0.0045	0.9995	0.00904
8	$y = 258.4x^3 - 453.1x^2 + 268.6x - 51.57$	0.0069	0.9978	0.01475

* x stands for $\log(F_r)$ and y stands for $\log(Q_m)$

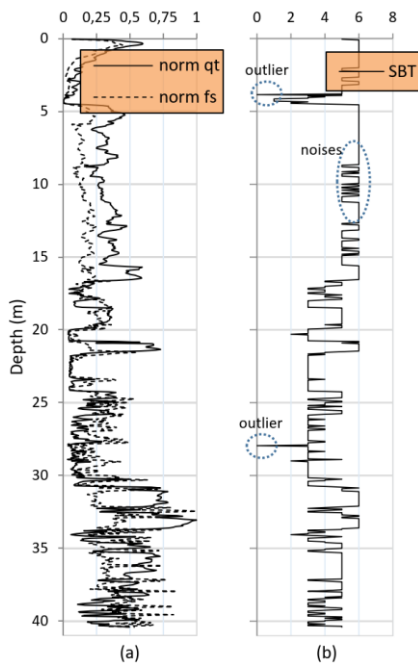


Figure 3: (a) The normalized corrected cone penetration resistance, q_t , and sleeve friction, f_s , of the CPT training database; and, (b) the identified SBT from the Robertson chart (1990)

$$\mu(x_i) \approx a_0 + a_1(x_i - x) + \frac{a_2}{2}(x_i - x)^2 \quad (2)$$

The local approximation can be fitted by locally weighted least squares, as in eq. 3. The coefficients estimates a_0 , a_1 and a_2 are chosen to minimize:

$$\sum_{i=1}^n W\left(\frac{x_i - x}{h}\right)(Y_i - \mu(x_i))^2 \quad (3)$$

A smooth weight function results in a smoother estimate (Macaulay, 1931). The tricube weight function was used in the LOESS (Locally Estimated Scatterplot Smoothing) fitting procedure (Cleveland, 1979):

$$w(u) = \begin{cases} \left(1 - \left|\frac{x_i - x}{h}\right|^3\right)^3 & |u| < 1 \\ 0 & |u| > 1 \end{cases} \quad (4)$$

w is a weight function with the following properties (Cleveland, 1979):

1. $w(x) > 0$ for $|x| < 1$;

2. $w(-x) = w(x)$;
3. $w(x)$ is a nonincreasing function for $x \geq 0$;
4. $w(x) = 0$ for $|x| \geq 1$.

It should be stated that in the present study, 10% of the data sets were considered as the bandwidth for calculation of the local regression in the LOESS method.

2.3. Nash-Harsanyi bargaining method

The Nash-Harsanyi bargaining model has been employed in different fields, especially in the environmental and water management studies (Madani, 2011; Farhadi et al., 2016; Fu et al., 2018).

As a game theory method, Nash (1953) proposed a bargaining model considering the cooperation among the players/decision-makers. This method maximizes the total product of members through coalition and cooperation, considering each member an equal proportion of cooperation. In spite, in the asymmetric Nash-Harsanyi bargaining model, the players share their different proportions of cooperation to obtain an agreement for the maximum overall benefit. Indeed, both the individual and also the collective rationalities are considered in this method (Fu et al., 2018).

In the Nash-Harsanyi bargaining model, n decision-makers with u_i objective functions, where i stands for each decision-maker, and d_i disagreement points take roles. The overall profit, Ω , in the model can be written as:

$$\Omega = \max \prod_{i=1}^n (u_i - d_i)^{p_i} \quad (5)$$

subject to:

$$u_i \geq d_i, i=1,2,\dots,n.$$

The main problem with the Robertson chart (1990) for stratification was probably estimating different SBTs for two adjacent data points which were close to each other, but located on different sides of a boundary line in the chart. Therefore, the proximity of the data points in the Robertson chart was considered as the basic for identification of strata. Hence, a distance criterion between the data points, named herein as N-H distance criterion, D_{N-H} , was introduced. Four decision-makers were considered as four N-H distance quantities: the distances between two succeeding data points, $d_{N-H(i,i-1)}$, with one

data point as interval, $d_{N-H(i,i-2)}$, with the interval of three data points, $d_{N-H(i,i-4)}$, and with the 9 data points interval, $d_{N-H(i,i-10)}$. Indeed, they were considered as the distance between the optimized solution and the disagreement point in the Nash-Harsanyi theory, i.e. (u_i-d_i) in eq. 5. If the powers p_i in eq. 5 were identified (which was computed through integrating the model with GWO), an N-H distance graph would be derived for the whole CPT log. For the identification of strata from the N-H distance graph, another distance criterion was defined, as α -cut distance, $D_{\alpha-cut}$. If the N-H distance for an interval of adjacent data points was higher than the α -cut distance, $D_{N-H} > D_{\alpha-cut}$, it would mean that there was a notable distance between the data points on the Robertson chart, and consequently, there

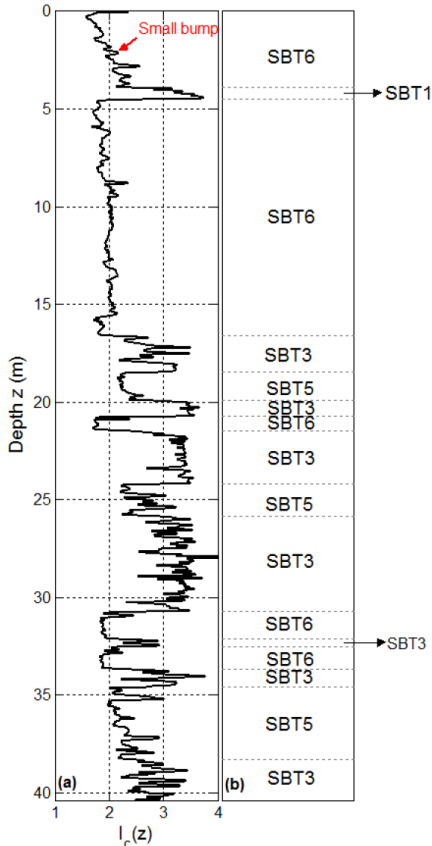


Figure 4: The SBT Index, I_c , and the identified stratification based on the experts' opinion (considered as the training database)

was a change in layer. Despite, if the N-H distance for a range of adjacent data points was lower than the α -cut distance, $D_{N-H} < D_{\alpha-cut}$, it would mean that the points were close to each other on the Robertson chart and there was a layer in that depth interval.

Nevertheless, the proportion of each decision-maker's cooperation, it means p_i , and the optimum α -cut distance, $D_{\alpha-cut}$, to reach the highest overall profit was unknown yet. The highest overall profit in this study was considered as the best stratification estimation the experts had for a CPT log, which is shown in Fig. 4. Therefore, an optimization method was integrated with the Nash-Harsanyi method to find the p_i and also $D_{\alpha-cut}$.

2.4. Grey Wolf Optimizer (GWO)

Mirjalili et al. (2014) proposed a meta-heuristic search algorithm inspired by grey wolves (*Canis lupus*). The algorithm has been employed in different fields like electric power system, soil mechanics, and image processing (Khairuzzaman and Chaudhury, 2017). It simulates the hunting process of grey wolves attacking a prey.

The social hierarchy of wolves is modelled mathematically considering alpha, α , beta, β , delta, δ , and omega, ω , wolves. The three best solutions are considered as α , β and δ wolves respectively, and the other possible solutions are considered as ω wolves. In a hunting (optimization) process, ω wolves follow the three best wolves.

In brief, different steps of hunting are modelled mathematically as below (Mirjalili et al., 2014):

- Encircling prey:

$$\vec{D} = \left| \vec{C} \cdot \vec{X}_p(t) - \vec{X}(t) \right| \quad (6)$$

$$\vec{X}(t+1) = \vec{X}_p(t) - \vec{A} \cdot \vec{D} \quad (7)$$

$$\vec{A} = 2\vec{a} \cdot \vec{r}_1 - \vec{a} \quad (8)$$

$$\vec{C} = 2 \cdot \vec{r}_2 \quad (9)$$

where, \vec{A} and \vec{C} are coefficient vectors, \vec{X}_p is the position vector of the prey, \vec{X} indicates the position vector of a grey wolf, \vec{r}_1 and \vec{r}_2 are random vectors in $[0,1]$, and \vec{a} vectors'

components are linearly decreased from 2 to 0 over the course of iterations.

- Hunting:

The alpha, beta, and delta wolves have better estimation of the potential solution and the omega wolves follow them. This is mathematically implemented as:

$$\begin{aligned}\bar{D}_\alpha &= \left| \bar{C}_1 \cdot \bar{X}_\alpha - \bar{X} \right| \\ \bar{D}_\beta &= \left| \bar{C}_2 \cdot \bar{X}_\beta - \bar{X} \right| \\ \bar{D}_\delta &= \left| \bar{C}_3 \cdot \bar{X}_\delta - \bar{X} \right|\end{aligned}\quad (10)$$

$$\begin{aligned}\bar{X}_1 &= \bar{X}_\alpha - \bar{A}_1 \cdot (\bar{D}_\alpha) \\ \bar{X}_2 &= \bar{X}_\beta - \bar{A}_2 \cdot (\bar{D}_\beta) \\ \bar{X}_3 &= \bar{X}_\delta - \bar{A}_3 \cdot (\bar{D}_\delta)\end{aligned}\quad (11)$$

$$\bar{X}(t+1) = \frac{\bar{X}_1 + \bar{X}_2 + \bar{X}_3}{3}\quad (12)$$

- Attacking prey:

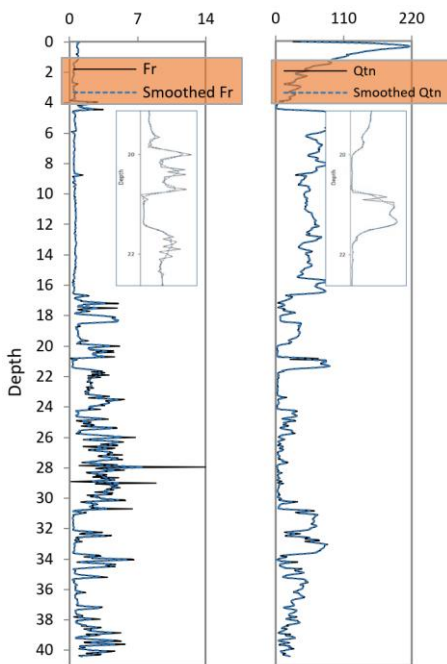


Figure 5: The normalized friction ratio, Fr , and normalized cone resistance, Q_m , data smoothed by the LOESS method

Approaching a prey is modelled by decreasing the value of \bar{a} over the course of iterations.

- Search for prey (exploration):

In order to avoid the local optimum finding, \bar{A} with random values greater than 1 and smaller than -1 oblige the search agent to diverge from the prey and search for the solution globally.

For the whole process of the GWO, as a pseudo-code, refer to Mirjalili et al. (2014).

The GWO was integrated with the Nash-Harsanyi model to find the optimum cooperation of decision-makers, i.e. p_i in eq. 5, and the $D_{\alpha-cut}$ distance based on the results of one CPT log as the training data. Clearly, if more CPT results will be introduced to optimize the parameters, it might become applicable to more types of soils in different regions.

3. Results and discussion

The smoothing LOESS method was applied to the normalized friction ratio, Fr , and normalized cone resistance, Q_m , data to relax the outliers' and uncertainties' impact. The results are illustrated in Fig. 5. A magnified part of the graph is also shown in the figure so that it might be easily seen how the data has changed. As can be seen, the whole data and the trends have not been changed after smoothing. But the outliers and the highly fluctuating points have become closer to the neighbouring points.

The integrated optimization-Game Theory model was applied to the smoothed data and the optimized quantities of p_1 , p_2 , p_3 , p_4 and $D_{\alpha-cut}$ were computed as 0.7992, 0.5472, 0.2115, 0.0019 and 0.0831, respectively. The optimization was performed based on the experts' stratification (Fig. 4). It was used as the training data, and the mean square error for the whole data was 0.5198. The estimated and the experts' stratification results are presented in Fig. 6. It should be noted that in the layers where $D_{N-H} > D_{\alpha-cut}$, the SBT has been considered according to the location of each data point on the Robertson chart because the variation of the succeeding data points on the chart were usually large, but for the layers between them, i.e. where the $D_{N-H} < D_{\alpha-cut}$, the average location of the data points on the Robertson chart was considered as the SBT of the layer.

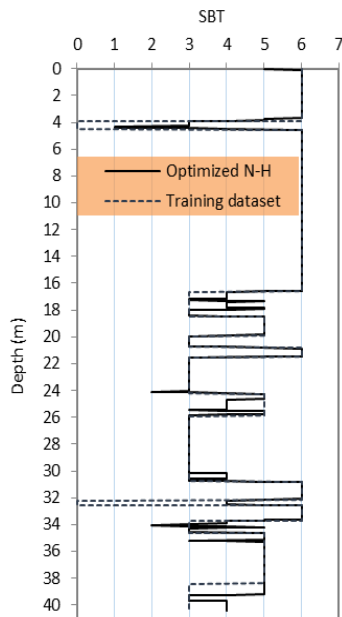


Figure 6: Comparison of the estimated and experts' stratification results for the training data

The proposed model was applied to three other CPT logs as the test data and the results are presented in Fig. 7.

4. Conclusions

A model based on the statistical and artificial

intelligence models was proposed to address the subground stratification based on CPT results. The outliers' and uncertainties' impact in CPT data was almost removed by the LOESS method, and the Nash-Harsanyi bargaining (as a Game Theory) model and Grey Wolf Optimizer (GWO) were integrated to identify the strata. The proposed model estimation of the stratification was comparable with the stratification proposed by experts.

Acknowledgements

I would like to appreciate Professor Tim Lämsivaara, Tampere University, Finland, helping me to write the paper and participate in this conference. Without his help, I couldn't really do it!

References

- Abraham, B., and Chuang, A. 1989. Outlier detection and time series modeling. *Technometrics*, 31(2).
- Anderson, T.W. 1971. *The statistical analysis of time series*. Wiley, New York.
- Cao, Z.J., Zheng, Sh., Li, D.Q., and Phoon, K.K. 2018. Bayesian identification of soil stratigraphy based on soil behaviour type index. *Canadian Geotechnical Journal*, 56(4): 570-586.
- Ching, J., Phoon, K.K., Li, K.H., and Weng, M.Ch. 2018. Multivariate Probability distribution for some intact rock properties. *Canadian Geotechnical*

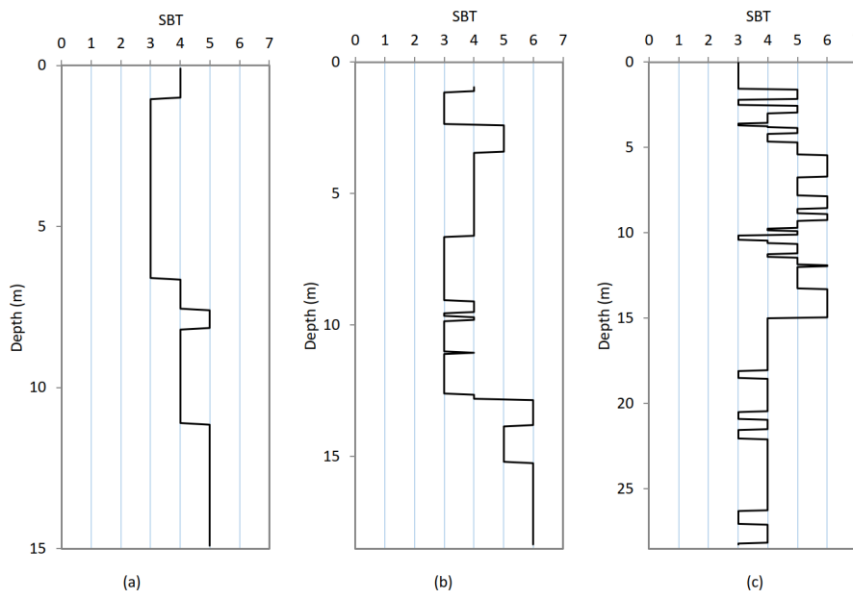


Figure 7: Application of the proposed model to the three data set: a, b and c

- Journal*, 56(8): 1080-1097.
- Ching, J., Wang, J.S., Juang, C.H., and Ku, C.S. 2015. CPT-based stratigraphic profiling using the wavelet transform modulus maxima method. *Canadian Geotechnical Journal*, 51 (12): 1993-2007.
- Cleveland, W.S. 1979. Robust locally weighted regression and smoothing scatterplots. *Journal of the American Statistical Association*, 74(368): 829-836.
- Das, S.K., and Basudhar, P.K. 2009. Utilization of self-organizing map and fuzzy clustering for site characterization using piezocone data. *Computers and Geotechnics*, 36: 241-248.
- D'Ignazio, M., Phoon, K.K., Tan, S.A., Länsivaara, T. 2016. Correlations for undrained shear strength of Finnish soft clays. *Canadian Geotechnical Journal*, 53(10): 1628-1645.
- Farhadi, S., Nikoo, M.R., Rakhshandehroo, Gh.R., Akhbari, M., and Alizadeh, M.R., 2016. An agent-based-nash modeling framework for sustainable groundwater management: A case study. *Journal of Agricultural Water Management*, 177: 348-358.
- Fu, J., Zhong, P.A., Zhu, F., Chen, J., Wu, Y. and Xu, B. 2018. Water resources allocation in transboundary river based on asymmetric Nash-Harsanyi Leader-Follower Game model. *Water*, 10(3).
- Hegazy, Y.A., and Mayne, P.W. 2002. Objective site characterization using clustering of piezocone data. *Journal of Geotechnical and Geoenvironmental Engineering*, 128: 986-996.
- Jung, B.-C., Gardoni, P., and Biscontin, G. 2008. Probabilistic soil identification based on cone penetration tests. *Geotechnique*, 58(7): 591-603.
- Kendall, M. and Ord, J.K. 1990. *Time series*, Oxford University Press, New York, third ed.
- Khairuzzaman, A.K., Chaudhury, S. 2017. Multilevel thresholding using grey wolf optimizer for image segmentation. *Experts Systems with Applications*. 86(15): 64-76.
- Li, J., Cassidy, M.J., Huang, J., Zhang, L., and Kelly, R. 2016. Probabilistic identification of soil stratification. *Geotechnique*, 66(1): 16-26.
- Ljung, G.M. 1993. On outlier detection in time series, *Journal of the Royal Statistical Society: Series B*, 55(2): 559-567.
- Loader, C. 1999. Local regression and Likelihood. *Statistics and computing*, Springer, New York, NY, <https://doi.org/10.1007/b98858>.
- Loader, C. 2012. Smoothing: Local Regression Techniques. In: Gentle J., Härdle W., Mori Y. (eds) *Handbook of Computational Statistics*. Springer Handbooks of Computational Statistics. Springer, Berlin, Heidelberg.
- Lunne, T., Eidsmoen, T., Gillespie, D., and Howland, J.D. 1986. Laboratory and field evaluation of cone penetrometers, Proceedings, *In-situ '86, ASCE Specialty Conference*, Blacksburg, Virginia, United States.
- Woollard, M., Storteboom, O., Länsivaara, T. and Selänpää, J. 2016. Additional parameters measured in a single CPT, click-on modules for the digital cone. In *5th International Conference on Geotechnical and Geophysical Site Characterisation: ICS'5*, Queensland, Australia.
- Macaulay, F.R. 1931. *Smoothing of time series*. New York, National Bureau of Economic Research.
- Madani, K. 2011. Hydropower licensing and climate change: Insights from cooperative game theory. *Advances in Water Resources*, 34(2): 174-183.
- Mirjalili, S.A., Mirjalili, S.M. and Lewis, A. 2014. Grey wolf optimizer. *Advances in Engineering Software*, 69: 46-61.
- Nash, J. 1953. Two-person cooperative games. *Econometrica*, 21: 128-140.
- Phoon, K.K., and Tang, Ch. 2019. Characterisation of geotechnical model uncertainty. *Georisk*, 13(2).
- Robertson, P.K. 1990. Soil classification using the cone penetration test. *Canadian Geotechnical Journal*, 27(1): 151-158.
- Robertson, P.K. 2009. Interpretation of cone penetration tests -a unified approach. *Canadian Geotechnical Journal*, 46(11): 1337-1355.
- Tonni, L. and Gottardi, G. 2011. Analysis and interpretation of piezocone data on the silty soils of the Venetian lagoon (Treporti test site). *Canadian Geotechnical Journal*, 48(4): 616-633.
- Wang, Y., Huang, K., and Cao, Z. 2013. Probabilistic identification of underground soil stratification using cone penetration tests. *Canadian Geotechnical Journal*, 50: 766-776.
- Zhang, Zh., and Tumay, M.T. 1999. Statistical to fuzzy approach toward CPT soil classification. *Journal of Geotechnical and Geoenvironmental Engineering*, 125: 179-186.